Inorganic Materials, Vol. 39, No. 6, 2003, pp. 539–554. Translated from Neorganicheskie Materialy, Vol. 39, No. 6, 2003, pp. 647–663.

Phase Equilibria in the Cu–Te System

A. S. Pashinkin* and V. A. Fedorov**

** Moscow State Institute of Electronic Engineering (Technical University), Zelenograd, Moscow, 103498 Russia*

*** Kurnakov Institute of General and Inorganic Chemistry, Russian Academy of Sciences, Leninskii pr. 31, Moscow, 119991 Russia*

e-mail: pgfed@igic.ras.ru

Received November 28, 2002; in final form, January 16, 2003

Abstract—The available phase-diagram data for the Cu–Te system are critically evaluated, and the *T–x* phase diagram is optimized. The thermodynamic properties, polymorphism, and crystal structures of copper tellurides are analyzed.

INTRODUCTION

The Cu–Te system is the most complex among the copper–chalcogen systems and has not yet been studied in sufficient detail. Data on this system were summarized earlier by Okamoto in 1994 [1]. The brief review by Feutelias and Legendre [2] cites, for the most part, data from [3]. In those works, not all Cu–Te phases are characterized, and thermodynamic data are lacking. In this paper, we present a critical evaluation of the available phase-diagram data for the Cu–Te system and summarize the thermodynamic properties of copper tellurides.

The Cu–Te system is interesting in that the most stable copper telluride Cu_2Te retains semiconducting properties in the liquid state [4]. Data on intermediate phases in the Cu–Te system are also of considerable interest in the context of the characterization of cupriferous electrolyte slime and tellurium extraction [5].

T–x PHASE DIAGRAM OF THE Cu–Te SYSTEM

The Cu–Te system was first studied in 1907. Puschin [6, 7] identified the compounds Cu_2Te and CuTe by measuring the room-temperature emf across the electrochemical cell $Cu/CuSO_4(aq)/Cu_xTe_{1-x}$. He observed a rather large change in emf (to 80–100 mV below the electrochemical potential of copper) in the composition range Cu_2Te–CuTe. Chikashige [8] studied the Cu–Te system using thermal and microstructural analysis. His results are presently of limited interest.

In the unpublished dissertation by Keymling [9], the *T–x* phase diagram of the Cu–Te system was studied in the composition range 0–66 at. % Te. That work was widely cited in later publications [10–12], which makes it possible to gain a general idea of his results. Later, Anderko and Schubert [12] mapped out the *T–x* phase diagram in the range 40–100 at. % Te using their own and earlier [8, 9] results.

The most comprehensive study of the copper–tellurium system was reported by Blachnik *et al.* in 1983 [13]. They used high-purity starting chemicals and carefully homogenized their samples by long-term annealing. The characterization techniques they used included differential thermal analysis (DTA), differential scanning calorimetry (DSC), and x-ray diffraction (XRD). Their findings form the basis of present-day knowledge of phase equilibria in the Cu–Te system [1, 2].

A drawback common to the aforementioned studies, except for the one by Chikashige [8], is the lack of numerical data in the form of tables. Experimental data were presented in the form of plots, occasionally even without data points [12]. The reported results do not always agree, even as to the compositions of intermediate phases, presumably because equilibration in the Cu–Te system requires anneals as long as several months [13]. Here, we assess the available results taking into account the latest reports.

Liquidus and binodals. The liquidus in the primary crystallization region of Cu was mapped out in [9]. Liquidus data in the range from Cu_2Te to 95 at. % Te were reported in [13]. The results obtained in those studies between 36 and 43 at. % Te coincide (Fig. 1). The liquidus line in the vicinity of Cu_2Te was constructed in [14] using precision DTA with an accuracy of ±1 K. In the range 33.3–36.0 at. % Te, the results reported by Blachnik *et al.* [13] and Glazov *et al.* [14] agree to within the experimental error. At the same time, the data reported by Glazov *et al.* [14] for the composition range 31.3–33.2 at. % Te are inconsistent with the position of the monotectic horizontal

$$L_2 \rightleftharpoons L_1 + Cu_2Te \quad (1)$$

reported in [13]. Thus, additional studies of the liquidus in region d_1f (Fig. 1) are needed.

0020-1685/03/3906-0539$25.00 © 2003 MAIK "Nauka/Interperiodica"

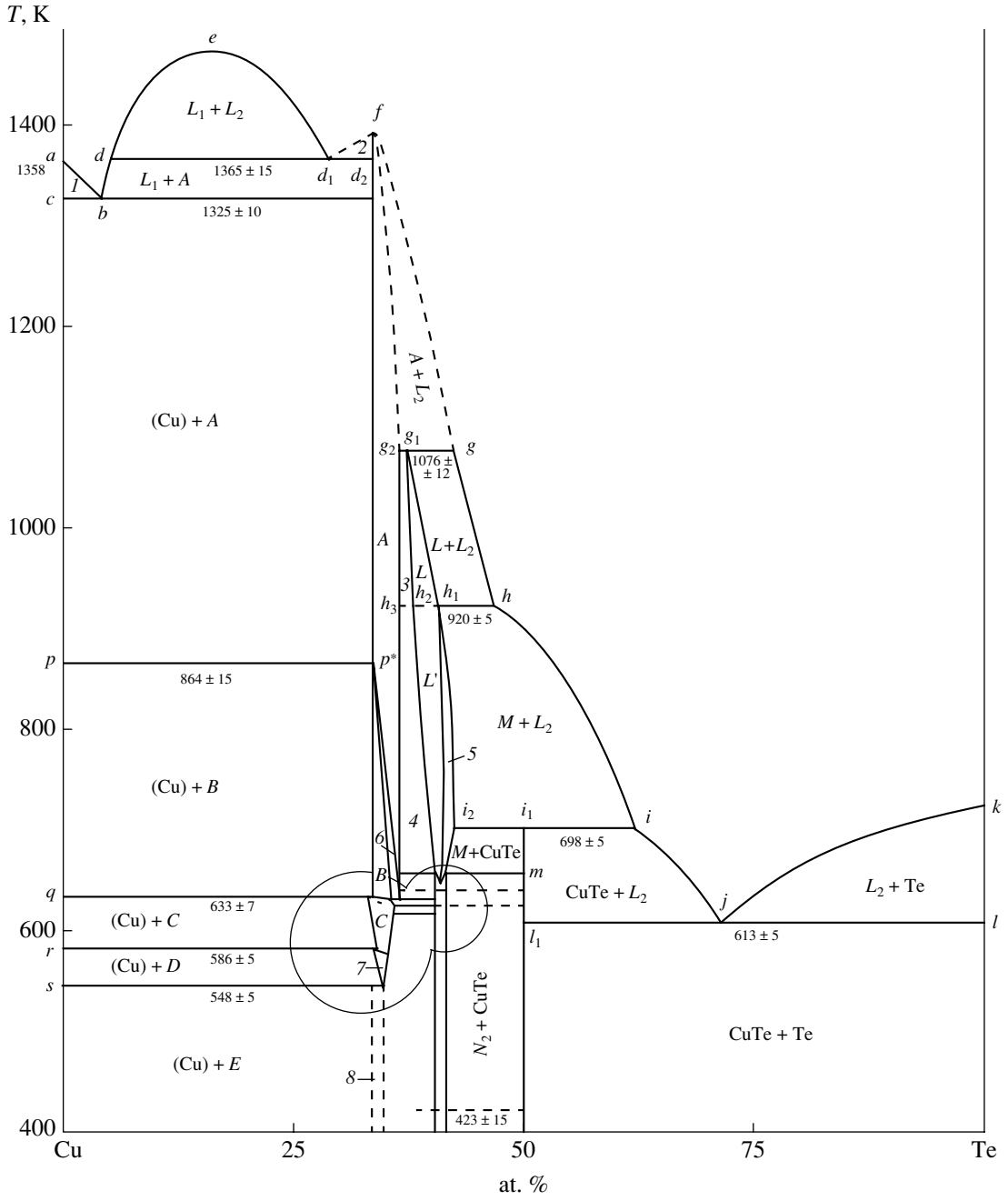

Fig. 1. *T–x* phase diagram of the Cu–Te system: (*1*) (Cu) + L_2, (*2*) L_2 + *A*, (*3*) *A* + *L*, (*4*) *A* + *L'*, (*5*) *M*, (*6*) *A* + *B*, (*7*) *D*, (*8*) *E*; designations are taken from [1]; because of the small scale, two points coincide at *p**.

The most detailed data on the miscibility gap between Cu and Cu_2Te (Fig. 1) were obtained in [15] by measuring the ultrasound velocity in the melt. Samples were prepared by slowly heating appropriate mixtures of electrolytic copper and TA-1 tellurium directly in the measuring cell, with 1-h halts at the melting points of the constituent components and melt stirring at 1600 K. The process was run in a spectral-grade argon atmosphere. The ultrasound velocity was measured repeatedly by a transducer translated vertically. Acoustic bonds were made by applying thin layers of boric anhydride to the transducer buffers. The temperature in the measuring cell was maintained with an accuracy of ±2–3 K. The critical point of the immiscibility dome was found to lie at 17.5 at. % Te and 1479 K [15].

Burylev *et al.* [16, 17] studied liquid immiscibility in the Cu–Te system by examining quenched materials. According to their results, the miscibility gap is bounded by essentially parallel lines. The most likely reason for the discordance between the results in ques-

Table 1. Melting point of Cu_2Te

T_m, K	Method	Source	T_m, K	Source
experimental data			recommendations	
~1400	Thermal analysis	[6]	≃1413	[3]
1384	DTA	[11]	≃1416	[1]
1390 ± 6	DTA	[13]	≃1413	[2]
1391 ± 1*	Precision DTA	[14]	1389.2	[14]
1387 ± 1**	Precision DTA	[14]	1388 ± 2	This paper

* Composition with T_{max} (33.7 ± 0.1 at. % Te).
** T_m of stoichiometric Cu_2Te.

tion is that, in the study by Burylev *et al.* [16, 17], the melt was equilibrated for an insufficient time. Therefore, their data should left out of consideration in constructing the equilibrium phase diagram.

Intermediate phases. The Cu–Te system contains seven compounds. Most of them exist in several different polymorphs, which were labeled *A* to *N* in [1], except for CuTe. Here, we also use those designations (Fig. 1). The only congruently melting compound is Cu_2Te.

Table 1 lists the experimentally determined and recommended melting points of *A*-Cu_2Te. Clearly, the melting temperature determined in [14] is the most reliable.

The heat of melting of Cu_2Te was determined by quantitative DTA (24.7 kJ/mol) in [18] and by drop calorimetry (9.95 ± 0.5 kJ/mol) in [19].

Glazov and Mendelevich [18] prepared Cu_2Te from stoichiometric mixtures of electrolytic copper (VCh grade) and 99.999%-pure tellurium. The mixtures were sealed in tubes under vacuum and heated over a period of 5 h with a 1-h halt at the melting point of tellurium. After the melting point of Cu_2Te was reached, the samples were furnace-cooled to 820 K and then quenched in water. Microstructural examination revealed the presence of small copper inclusions, which were also observed in later studies [20].

Blachnik and Gunia [19] prepared Cu_2Te from semiconductor-grade copper and tellurium. Stoichiometric mixtures were sealed in silica tubes under vacuum and heated stepwise to 20–35 K above the melting point of Cu_2Te. The samples were cooled for 3 weeks.

Although the reported heats of melting differ by a factor of 2.5, it is difficult to give preference to one of them. There is however some evidence in favor of the value obtained in [18]. First, Glazov and Mendelevich [18] found the entropy of melting of M_2X (M = Cu, Ag) calculated from their $\Delta_m H$ data to be strongly correlated with the bond ionicity in these chalcogenides, in contrast to the $\Delta_m S$ values obtained in [19]. Second, Glazov *et al.* [14], using the experimentally determined melting temperature and heat of melting of Cu_2Te and the calculated radius of curvature of the liquidus line at the melting point of Cu_2Te [18], assessed the dissociation of Cu_5Te_3 in the melt. The presence of this compound in the melt may be interpreted as indicating that even more complex tellurides are present in the solid phase [1].

The thermal dissociation of Cu_5Te_3 is likely to occur according to the scheme

$$Cu_5Te_3 \rightleftharpoons 2CuTe + 3Cu + Te. \quad (2)$$

The Te activities calculated for process (2) and Te contents from 32 to 38 at. % agree well with the experimentally determined values [21, 22]. Nevertheless, it is desirable to redetermine the heat of melting of Cu_2Te.

$Cu_{2-x}Te$ has a rather broad homogeneity range (Figs. 1, 2). According to Blachnik *et al.* [13], at 400 K it exists between 33.5 and 36.2 at. % Te. With increasing temperature, the extent of the homogeneity range slightly increases. According to Glazov *et al.* [20], the homogeneity range of this phase at 473 K is 33.3–37.5 at. % Te.

Near the melting point, the homogeneity range of $Cu_{2-x}Te$ includes the stoichiometric composition Cu_2Te [14]. At the same time, stoichiometric samples quenched from 50 K below the melting point contain needlelike Cu precipitates. Therefore, the location of the Cu-rich phase boundary of $Cu_{2-x}Te$ at the composition Cu_2Te is questionable.

Comparison of the Cu-rich phase boundary of $Cu_{2-x}Te$ in Fig. 1 with the data obtained in [20] leads us to assume that, above the eutectic temperature (1323 K), this boundary has a retrograde character. The partial phase diagram displayed in Fig. 2 indicates that, below ≃700–800 K, the Cu-rich phase boundary is shifted from Cu_2Te to more Te-rich compositions by about 0.2 at. %.

Below ≃720 K, the Cu-rich phase boundary of $Cu_{2-x}Te$ lies at 33.3–33.7 at. % Te. Data on the Te-rich

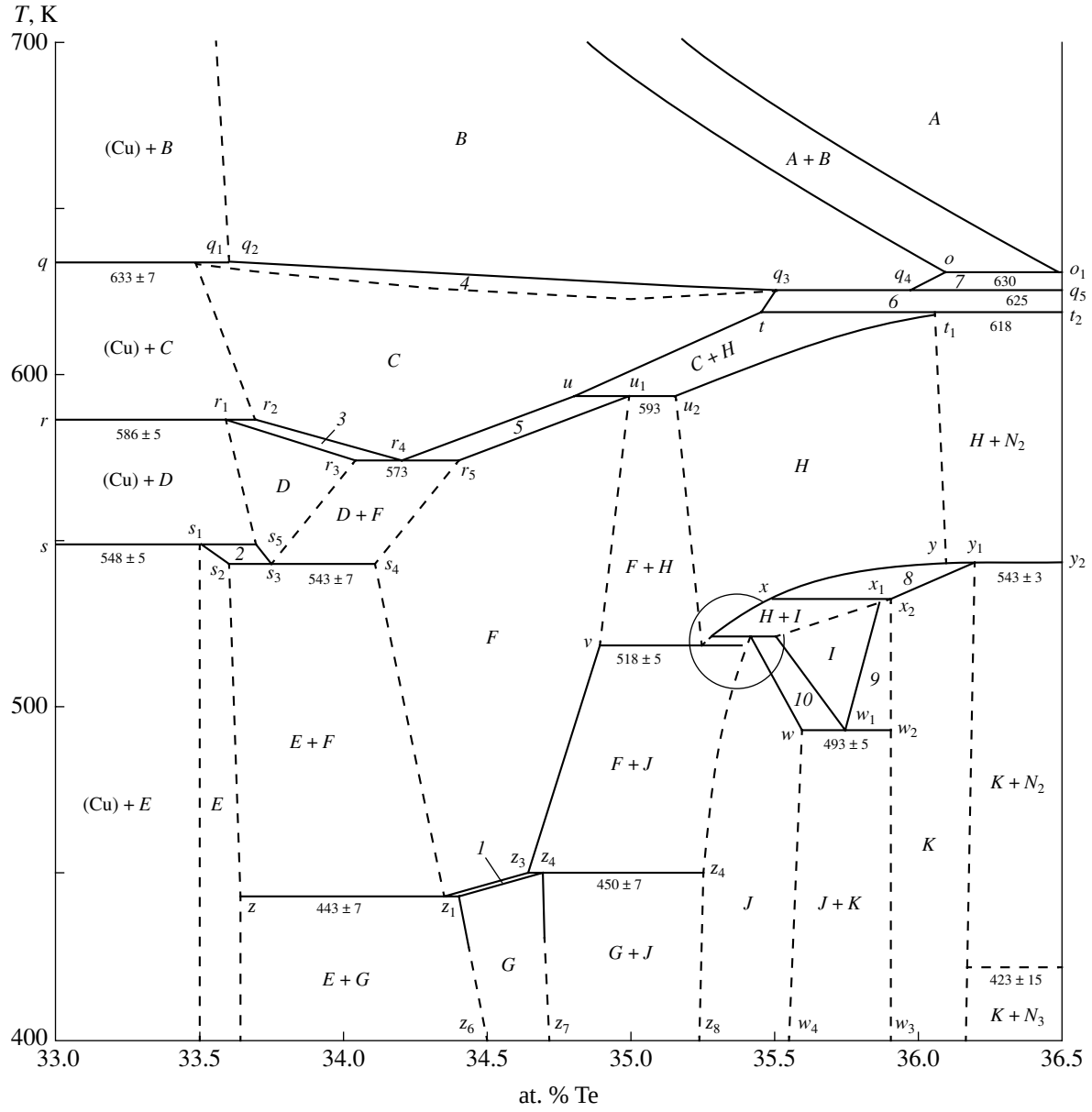

Fig. 2. Partial *T*–*x* phase diagram of the Cu–Te system in the range 400–700 K at Te contents from 33 to 36.5 at. %: (*1*) *F* + *G*, (*2*) *D* + *E*, (*3*) *D* + *C*, (*4*) *B* + *C*, (*5*) *C* + *F*, (*6*) *C* + N_2, (*7*) *B* + N_1, (*8*) *H* + *K*, (*9*) *I* + *K*, (*10*) *I* + *J*.

phase boundary are less accurate, and its shape can be judged from Fig. 1.

The Cu_2Te phase region has a rather complex shape. First, this compound exists in five different polymorphs: *A*–*E* [1–3, 9, 12]. Second, in the range 290–590 K, it participates in a number of peritectoid and eutectoid reactions, leading to the formation of the *F*, *H*, and *I* phases, which are only stable at elevated temperatures, and the *G*, *J*, *K*, and *N* phases, which exist at room temperature in single-phase form or in equilibrium with other phases (Fig. 2) [2, 13].

A similar single-phase region was reported for $Cu_{2-x}S$ [23]. At the same time, $Cu_{2-x}Se$ exists in only two polymorphs [24]. The systematic variation in the number of polymorphs and the configuration of the single-phase region of $Cu_{2-x}X$ in going from S to Se and to Te provides clear evidence of secondary periodicity in the copper chalcogenide series.

The DTA, DSC, and XRD data obtained in [13] and the DTA and coulometric titration data obtained in [25] were used to construct a partial phase diagram near $Cu_{2-x}Te$ between 373 and 680 K (Fig. 2). The results of those studies are in perfect agreement. Moreover, the DTA data obtained in [25] agree with other results [13, 26].

The low-temperature boundary of *A*-Cu_2Te is the solidus line p_1o_1 (Figs. 1, 2). The narrow two-phase

region p_1o_1o separates the *A* and *B* forms of Cu_2Te. These boundaries were located using, for the most part, data from [13, 26]. *B*-Cu_2Te exists in a small triangular region (Fig. 2). This phase has the largest extent, from 34.0 to 35.9 at. % Te, between 630 and 635 K. The two-phase region $B + C$ is vanishingly narrow [13, 25]. The phase field of the lower temperature phase *C*-Cu_2Te is bounded by lines of three-phase equilibria involving *D*-Cu_2Te and *E*-Cu_2Te at more Cu-rich composition and the *F* and *H* phases at more Te-rich compositions. On cooling, the last two phases transform into the low-temperature phases *G*, *J*, and *K* (Figs. 2, 3).

Thus, the homogeneity range, as broad as ≃3 at. % for *A*-Cu_2Te, becomes markedly narrower in going to *B*-Cu_2Te and *C*-Cu_2Te and becomes very narrow as these phases transform into *D*-Cu_2Te and *E*-Cu_2Te at 550–573 K.

D-Cu_2Te exists in a triangular region (Fig. 2) between 33.7–34.05 and 33.75 at. % Te. The last value corresponds to the formula $Cu_{1.96}Te$. The transformation (Cu) + $C \rightleftharpoons E$ is of a peritectoid type [2, 3].

The low-temperature phase *E*-Cu_2Te has a very narrow homogeneity range, from 33.49 to 33.64 at. % Cu (Fig. 2). Its composition is close to $Cu_{1.98}Te$. This phase forms by the peritectoid reaction (Cu) + $D \longrightarrow E$. The transformation temperature, 548 ± 3 K, was determined accurately in [13, 26] by studying the corresponding region of the *T–x* phase diagram (Fig. 2). This value agrees well with the ≃550 K recommended in [1]. The *E*-Cu_2Te phase field is located only tentatively.

The mutual transformations of the *D*, *F*, and *H* phases are well seen in Fig. 2. The *F* and *G* phases seem to be different polymorphs of the same compound since they are close in composition to $Cu_{13+x}Te_7$.

The *H* phase ($Cu_{9\pm x}Te_5$) is closely related to three other phases: *I* (≃Cu_9Te_5), *J* ($Cu_{9\pm x}Te_5$), and *K*. The composition of the last phase is Cu_7Te_4. The *J* and *K* phases form eutectoidally from the *I* phase.

The compound Cu_4Te_3 (42.9 at. % Te) was mentioned in [8–11] and later in [27]. It was reported to exist in two polymorphs. In later studies [28–30], the composition of the phase intermediate between $Cu_{2-x}Te$ and CuTe was assumed to be $Cu_{3-x}Te_2$ (40.5–40.8 at. % Te). Their results were confirmed in [13] and were cited in [1–3].

The homogeneity range and phase transformations of $Cu_{3-x}Te_2$ were considered in [1], but only the data obtained in [13] were cited. Here, we consider this phase in greater detail.

In Okamoto's notation [1], $Cu_{3-x}Te_3$ exists in four phase fields: *N*, *M*, *L*', and *L* (Fig. 4). Note that equilibration in the composition range near $Cu_{3-x}Te_2$ requires a long time. For example, according to Blachnik *et al.* [13] a composition corresponding to the *L*' phase could not be brought to equilibrium by annealing at 770 K for as long as 6 months: XRD analysis showed

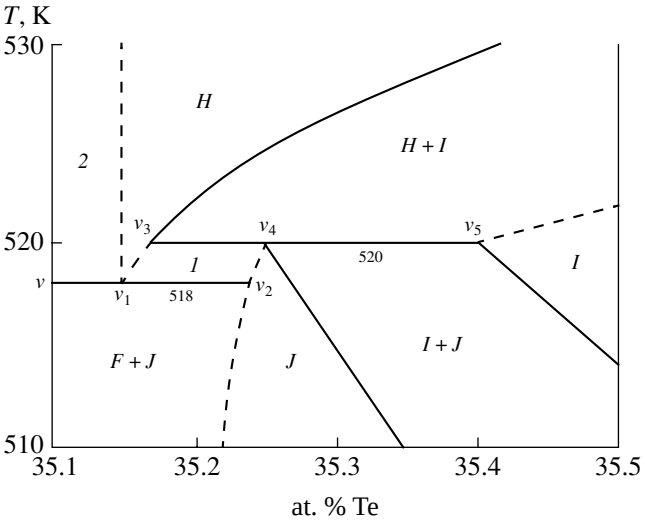

Fig. 3. Partial *T–x* phase diagram of the Cu–Te system in the range 510–530 K at Te contents from 35.1 to 35.5 at. % (circled region in Fig. 2): (*1*) $H + J$, (*2*) $F + H$; the compositions along the two boundaries of the *H* phase region are taken from [1].

that the sample consisted of $Cu_{3-x}Te_2$, $Cu_{2-x}Te$, and CuTe.

The *N* phase region extends from 40.0 to 41.5 at. % Te [1, 13]. According to Stevels [29], the *N* phase exists in a somewhat broader range, from 40.0 to 42.2 at. % Te (<663 K), while Misota *et al.* [28] reported a narrower range, from 40.8 to 41.5 at. % Te (473 K). Since the results reported in [13] were obtained later than those in [28, 29], preference should be given to the data in [2, 13]. Above 653 K, the *N* phase is unstable and transforms in the *L*' and *M* phases (see section *Three-phase equilibria* for more details).

The homogeneity range of the *M* phase is no broader than ≃1 at. % [1]. At 673 K, this phase exists between 41.15 and 41.8 at. % Te [13]. According to coulometric studies [31], the *M* phase region extends from 41.14 to 41.48 at. % Te. Thus, the data obtained in [13, 31] are in perfect agreement.

The *M* phase melts incongruently above 929 K [1, 13]. No $M + L'$ or $M + L$ two-phase regions were reported in [1, 2, 13]. It is not yet clear whether this is due to the structural similarity between the phases involved or the vanishingly small width of the fields in question.

The low-temperature boundary of the *L*' phase is determined by two three-phase equilibria: $L' \rightleftharpoons N + M$ (643 K) and $A + L' \rightleftharpoons N$ (653 K) [1, 13]. The largest width of the *L*' phase field near the equilibrium $L \rightleftharpoons L'$ is 3 at. % [1, 13]. The temperature of the $L \rightleftharpoons L'$ transformation is 920 ± 4 K according to Blachnik *et al.* [13] and 918 K according to Okamoto [1]. This transformation was also reported to occur at 903 [12, 27, 29] or 898–908 K [9]. We give preference to the value recommended in [1]. Note that no $L + L'$ two-phase region

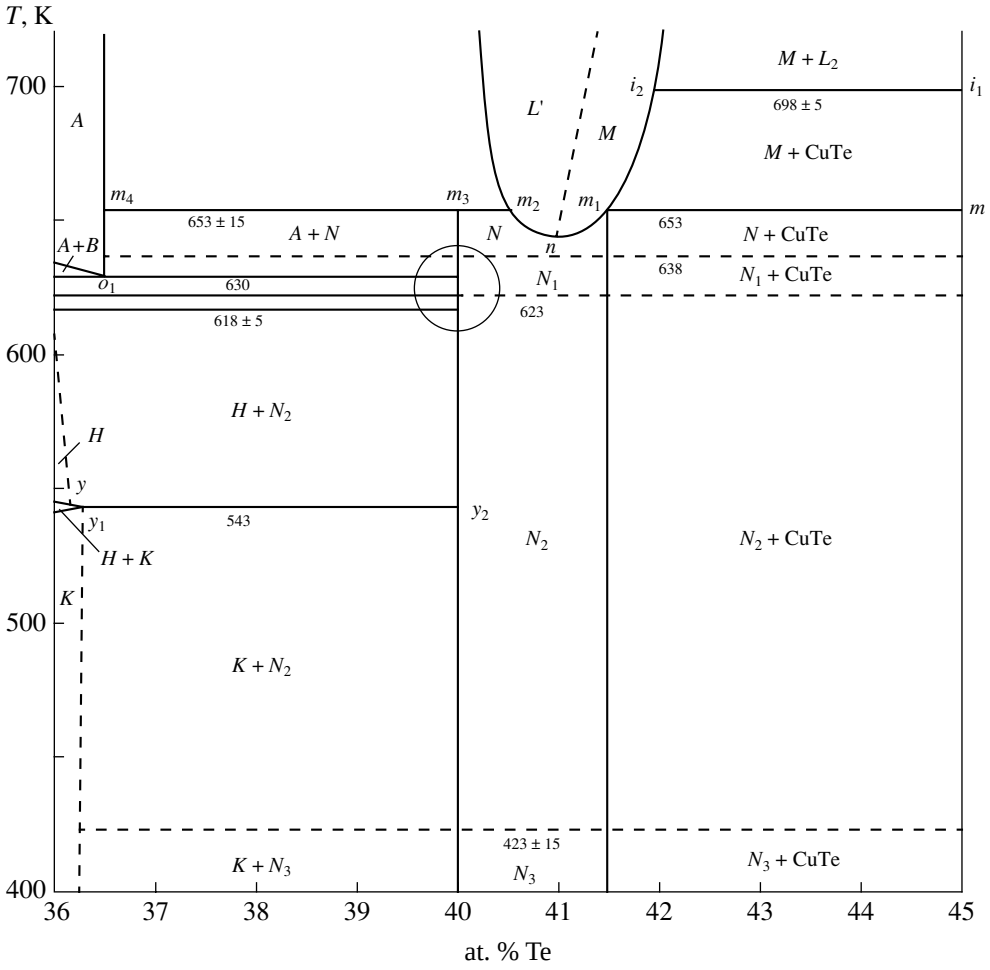

Fig. 4. Partial *T–x* phase diagram of the Cu–Te system in the range 400–720 K at Te contents from 36 to 45 at. %. Detailed phase equilibria in the circled region are displayed in Fig. 5. The $C + N_1$ field is not indicated (see Fig. 5).

was detected in phase-diagram studies. The high-temperature phase *L* was reported to melt incongruently at 1075 ± 11 [13] or 1083 K [1]. The latter value appears more reliable.

The phase transformations of $Cu_{3-x}Te_2$ below 643–653 K (field *N*) are the most difficult to analyze. These transformations were found in [12, 13, 27, 29, 32] but were not discussed in [3]. Here, we indicate the temperatures and heats of these transformations. The crystal chemistry of the phases involved will be considered below.

Figure 5 shows the partial phase diagram of the Cu–Te system near the *N* phase, constructed with allowance for the recommendations in [1]. The polymorphic transformations of these phase are shown schematically because the information available in the literature is insufficient for identifying their nature. Three polymorphic transformations of the *N* phase were identified with certainty, those at 423 ± 15, 623 ± 2 [13, 27–29], and 638 K [28, 29].

The temperature of the $N_3 \rightleftharpoons N_2$ transformation (Fig. 4), identified in [28, 29, 32], is worthy of special mention. Stevels [29] interpreted the disappearance of superlattice reflections at 413 K (41.4 at. % Te) as evidence of a second-order phase transition. According to DTA data [28], this transition occurs at ≃400 K, as evidenced by a weak, broad peak. Burmeister [32] observed an endothermic event at 423 K ($Cu_{3-x}Te_2$ + CuTe two-phase region). The average of these results is 423 ± 15 K.

Not all thermal events corresponding to this region of the *T–x* phase diagram (Fig. 4) can be interpreted unambiguously. For example, according to Anderko and Schubert [12], the heating curve of a sample containing 42.8 at. % Te (*N* + CuTe field) showed an endotherm at 638 K, that is, intermediate in temperature between the equilibria $N \rightleftharpoons M + L'$ and $N \rightleftharpoons N_1$ (Fig. 4). Most likely, the endotherm results from the overlap of the two transformations. The events observed at 613 [27] and 573 K [32] (42.8 at. % Te) are also difficult to interpret.

The heats of a number of transformations were determined by DTA and DSC. For example, the thermal effect of the reaction $L' + M \rightleftharpoons N$ is 27.2 kJ/mol [32].

The thermal effect of the $N \rightleftharpoons N_1$ phase transformation (633 K) is 25.1 kJ/mol. Data for the $N_1 \rightleftharpoons N_2$ transformation (623 K) are contradictory: the heat of this transition is 4.2 kJ/mol according to Stevels [29] and 13 kJ/mol according to Sharma and Selekna [27]. We believe that the former result is more reliable.

Blachnik *et al.* [13] call attention to the complexity of phase equilibria in the composition region in question and cite the report by Colaitis *et al.* [33], who identified complex structures of $Cu_{3-x}Te_2$, including shear structures and polytypes, using electron diffraction and electron microscopy. These structures, however, were not correlated with the phase relations in the Cu–Te system.

Copper monotelluride, CuTe, was first identified by emf measurements [6, 7] and later by XRD and microstructural analysis [12]. CuTe melts incongruently by the reaction $CuTe \longrightarrow M + L_2$ [13] (Table 2).

The recommendations in [1] coincide with the results obtained in [13]. We take the incongruent melting temperature of CuTe reported in [13]: 698 ± 5 K.

Copper ditelluride, Cu_2Te, has the pyrite structure. At 6.5 GPa, its temperature stability range is 373–1473 K [1, 34]. At 3.3 GPa, Cu_2Te forms at 773 K by the reaction [34]

$$2Cu_2Te \longrightarrow CuTe_2 + 3Cu. \quad (3)$$

At atmospheric pressure, copper ditelluride is unstable.

Cu- AND Te-BASED SOLID SOLUTIONS

Smart and Smith [35] determined the limit of the Cu-based solid solution from electrical conductivity measurements in the range 873–1073 K. Their data were used to derive the equation of the solvus line for the solubility of *A*-Cu_2Te in Cu from 873 to 1073 K. The lower temperature is very close to the temperature of the $A \rightleftharpoons B$ transformation of Cu_2Te. The solubility of Cu_2Te in Cu rises with temperature according to the equation

$$\log x = -7372/T + 2.43, \quad (4)$$

where x is the mole fraction of Cu_2Te dissolved in solid copper.

From this equation, the heat of solution of Cu_2Te in Cu is 141 ± 3 kJ/mol.

According to Eborall [36], the Cu_2Te solubility in Cu at 1073 K is much lower than 0.02 at. %. This estimate is consistent with the results obtained in [35] but is only tentative because the copper used in [36] contained 0.03 at. % P.

Data on CuTe solubility in solid Te are missing.

THREE-PHASE EQUILIBRIA

Many of the three-phase, invariant equilibria in the Cu–Te system are clear from the above discussion and the data presented in Figs. 1–4. Since the Cu–Te system has been studied for almost 100 years, there are some contradictions in the reported results, which led us to evaluate the three-phase equilibria in this system. For this purpose, it is convenient to represent available data in the form of tables, as was done in [1], where all three-phase equilibria were summarized in one table with brief comments. In our opinion, it is more convenient to display three-phase equilibria in two tables, one corresponding to Fig. 1 (entire *T–x* phase diagram of the Cu–Te system) (Table 3), and the other corresponding to Figs. 2–4 (finer details of the phase diagram) (Table 4).

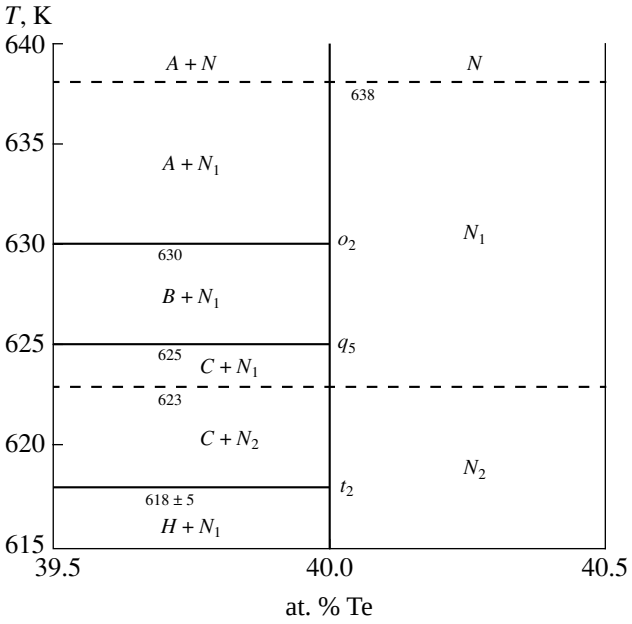

Fig. 5. Partial *T–x* phase diagram of the Cu–Te system in the range 615–640 K at Te contents from 39.5 to 40.5 at. %.

Tables 3 and 4 are based on the results reported in [13, 28] and recommendations in [1]. Also indicated are studies confirming the data from [1, 13, 28]. Some of the data presented in [28], mainly those obtained below 440 K, are not included in Table 4, because the equilibrium state was hardly reached at these low temperatures.

***T–x* phase diagram of the Cu–Te system.** Detailed analysis of the three-phase equilibria in the copper–tel-

Table 2. Reported temperatures of the reaction $CuTe \longrightarrow M + L_2$

T, K	Reference	*T*, K	Reference
640	[9]	689 ± 5	[13]
638	[12]	698*	[1]
613	[29]		

* Our recommendation.

Table 3. Three-phase equilibria in the Cu–Te system (Fig. 1)

Equilibrium	Te content of the phases involved, at. %			*T*, K	Type of equilibrium	Reference
$L_2 \rightleftarrows L_1 + A$	29	5	33.3	1365 ± 15	Monotectic	[1–3, 13]
$L_1 \rightleftarrows$ (Cu) + A	4.6	≃0.07	33.3	1325 ± 10	Eutectic	[1–3, 9, 13]
(Cu) + $A \rightleftarrows B$	1×10^{-4}	33.3	33.3	864 ± 15	Peritectoid	[13]
(Cu) + $B \rightleftarrows C$	≃0	≃33.6	≃33.6	633 ± 7	Peritectoid	[2, 6, 9, 13]
(Cu) + $C \rightleftarrows D$	≃0	≃33.7	33.7	586 ± 5	Peritectoid	[2 6, 9, 13]
(Cu) + $D \rightleftarrows E$	≃0	33.7	33.5	548 ± 15	Peritectoid	[2, 13]
$L_2 + A \rightleftarrows L$	43	36.5	37	1076 ± 12	Peritectoid	[2, 13]
$L_2 + L \rightleftarrows M$	47	41	41	920 ± 5	Peritectoid	[2, 13]
$L_2 + M \rightleftarrows$ CuTe	67	42	50	698 ± 3	Peritectoid	[2, 13]
$L_2 \rightleftarrows$ CuTe + Te	71	50	0	613 ± 3	Eutectic	[2, 13]
$A + L' \rightleftarrows N$	36.5	40.5	40	653 ± 15	Peritectoid	[1]*
$M \rightleftarrows N$ + CuTe	41.5	41.5	40	653	Eutectic	[1]

* According to Feutelias and Legendre [2], the temperature of this three-phase equilibrium is 633 K.

Table 4. Three-phase equilibria in the Cu–Te system (Figs. 2–4)

Equilibrium	Te content of the phases involved, at. %			*T*, K	Type of equilibrium	Reference
$A \rightleftarrows B + N_1$	36.5	35.9	40	630 ± 5	Eutectoid	[1, 13]
$B \rightleftarrows C + N_1$	35.95	35.5	40	625 ± 5	Eutectoid	[1, 13, 25]
$C + N_2 \rightleftarrows H$	35.45	40	36.05	618 ± 5	Peritectoid	[1, 13, 25]
$C + H \rightleftarrows F$	34.8	35.15	35	593 ± 5	Peritectoid	[1, 13, 25]
$C \rightleftarrows D + F$	34.2	34.05	34.4	573 ± 5	Eutectoid	[1, 13, 25, 26]
$D \rightleftarrows E + F$	33.75	33.65	31.4	543 ± 7	Eutectoid	[1, 11, 13, 29]
$H + N_2 \rightleftarrows K$	36.1	40	36.7	543 ± 3	Peritectoid	[1, 13]
$F \rightleftarrows E + G$	34.35	33.65	34.4	443 ± 7	Eutectoid	[1, 13, 26]
$F + J \rightleftarrows G$	34.65	35.25	34.7	450 ± 7	Peritectoid	[1, 13, 29]
$H \rightleftarrows F + J$	35.2	34.9	35.25	518 ± 5	Eutectoid	[2, 3, 11, 13, 25]
$H + I \rightleftarrows J$	35.15	35.4	35.25	520 ± 5	Peritectoid	[1, 2, 13]
$H + K \rightleftarrows I$	35.55	35.9	35.85	533 ± 5	Peritectoid	[1, 13, 25]
$I \rightleftarrows J + K$	35.75	35.6	35.9	493 ± 5	Eutectoid	[1, 13, 25]
A, N, N_1	36.5	40	40	638	–	[28, 29]*
N, N_1, CuTe	41.5	41.5	50	638	–	[28, 29]*
C, N_1, N_2	35.5	40	40	623	–	[13, 27–29]*
N_1, N_2, CuTe	41.5	41.5	50	623	–	[13, 27–29]*
K, N_2, N_3	36.25	40	40	423 ± 15	–	[28, 29]*
N_2, N_3, CuTe	41.5	41.5	50	423 ± 15	–	[28, 29]*

* Our recommendations; the type of these equilibria cannot be identified with certainty.

lurium system allowed us to map out as complete a T–x phase diagram as possible (Figs. 1–5). Figure 1 shows the entire phase diagram, where the arrangement of large and medium phase fields is well seen. Figures 2–5 highlight finer details of phase relations. Some of the two-phase regions are very narrow (Figs. 2, 3).

Note also that the temperature of the $N_1 \rightleftharpoons N_2$ polymorphic transformation (623 K) is essentially identical to the temperature of the equilibrium $A \rightleftharpoons B + M$ (Figs. 4, 5). For this reason, only the line of this three-phase equilibrium is shown in Fig. 2.

The three-phase equilibrium $L' \rightleftharpoons N + M$ [1] is actually represented by a point (Fig. 4), as confirmed by the facts that the composition range of this equilibrium is no broader than 0.5 at. % and that the location of point N was indicated in [1] with a large uncertainty.

The temperature of the $A + L' \rightleftharpoons N$ phase transformation in Table 1 differs from that in Fig. 1 in [1]. The temperature given in this work (653 K) is taken from Table 1 in [3] but is indicated with large error limits (±15 K).

In constructing the phase diagram, we used the melting point of copper reported in [37] (1357.65 ± 0.5 K) and that of tellurium reported in [38] (722.9 ± 0.1 K). The heat of melting of the CuTe–Te eutectic is 9.09 ± 0.14 kJ/mol [39].

The eutectic and monotectic temperatures in the partial system Cu–Cu_2Te are worthy of special mention. In this review, we rely on the results reported in [13] and recommendations made in [1]. Note that the temperatures of these equilibria given in [2, 3] coincide with those determined in [13]. In earlier reports, the separation between the monotectic and eutectic lines in this region was much smaller: from several kelvins [9, 10] to 1 K [36]. The origin of this discrepancy has not been discussed in the literature. It cannot be ruled out that Blachnik *et al.* [13] used purer starting chemicals, which raised the melt separation temperature by about 40 K.

CRYSTAL STRUCTURES OF COPPER TELLURIDES

The crystal structures of intermediate phases in the Cu–Te system were summarized by Okamoto [1], who limited his consideration to listing recommended space groups and homogeneity ranges. He also presented a large body of data on lattice parameters, without, however, specifying recommended values, pointing out that later results appear more reliable. The I, L, and L' phases have not been characterized by XRD. The information reported in [3] allows one to assess the reliability of the reported lattice parameters of intermediate phases relying on the recommendations made in [40] and the results obtained in [13]. The lattice parameter c of the C phase reported in [1, 13, 41, 42] differs from that obtained in [13, 40] by a factor of 3 to 5, pointing to structural ordering. Superstructures were also reported for the K, N_2, and N_3 phases (Table 5).

The reason for the formation of superstructures is that all of the phases in the Cu–Te system (A–N) consist of a rigid Te framework and mobile copper ions in different valence states, Cu(I) or Cu(II). The arrangement of the Cu ions depends on the composition of the phase and thermal history, which may lead to the formation of a superstructure [29, 41, 42, 45]. Stevels [29] and Patzak [44] pointed out that the lattice parameters a_{hex} and c_{hex} can be related to a_{cub} of the A phase. According to Stevels [29], $a_{hex} \simeq \frac{\sqrt{2}}{2} a_{cub}$ and $c_{hex} \simeq \frac{2\sqrt{3}}{3} a_{cub}$.

In electron diffraction studies of $Cu_{3-x}Te_2$ films (mainly the N_2 phase), Colaitis *et al.* [33] revealed a large number of superstructures which had a polytype character, with lattice parameters being multiples of a_{tetr}: $18a_{tetr}$, $23a_{tetr}$, $31a_{tetr}$, and $88a_{tetr}$. These structures, however, were not correlated with the phase relations in the Cu–Te system near $Cu_{3-x}Te_2$.

For a number of phases, the composition dependences of lattice parameters were reported. The lattice parameters of the B phase at 650 K were found to follow Vegard's law in the range 33.3–36.1 at. % Te [13], while the lattice parameters of the N_3 phase vary nonlinearly with composition [28].

According to Stevels [29], the M phase has a cubic structure. This, however, was not confirmed in later, more detailed studies [13]. The structure of this phase has not yet been identified with certainty.

As is seen from Table 5, the lattice parameters of one of the superstructures to the C phase coincide with those of the H phase, which was left out of consideration in [1]. Moreover, the lattice parameters of the H phase (Table 5) are identical to those of the K phase [42]. To understand the origin of these coincidences, additional structural studies must be carried out on samples prepared by carefully controlled procedures, followed by long-term annealing and rapid quenching.

THERMODYNAMIC CHARACTERISTICS OF COPPER TELLURIDES

Standard heats of formation and standard entropies were reported only for $Cu_{2-x}Te$, $Cu_{3-x}Te_2$, and CuTe. The techniques by which they were determined and the reliability of the data will be considered below. Note that the heat of formation of $Cu_{2-x}Te$ was determined by several methods, including tin calorimetry at 700 K [46, 47]. To calculate the standard heat of formation of this phase, one should know the heat capacity of copper, tellurium, and copper telluride because $Cu_{2-x}Te$ exists in a large number of polymorphs.

Heat capacity of copper tellurides. Heat capacity data are available only for $Cu_{2-x}Te$ and CuTe. Low-temperature heat capacity measurements were carried

Table 5. Structures of intermediate phases in the Cu–Te system

Phase	at. % Te	*T*, K	Structure	Sp. gr.	Lattice parameters, Å			Ref.	Note
					a	*b*	*c*		
$Cu_{2-x}Te$									
A	36.3	298	Cubic	*Fd*3*m*	6.03	–	–	[1, 13]	
B	33.3	298	Hex.	*P*6/*mmm*	4.246	–	7.289	[1, 40]	Cu_2Te, weissite
C	33.3	298	Hex.	–	8.37	–	21.60	[41, 42]	
C	35.0	298	Hex.	–	8.53	–	36.03	[1, 13]	
D	34.0	573	Orthorh.	–	4.227	7.403	7.290	[1, 29]	
E	33.7	298	Orthorh.	–	7.319	22.236	36.458	[1, 40]	
Phases resulting from decomposition of the *C* and *D* phases									
F	34.0	293	Orthorh.	–	7.189	4.187	7.207	[1, 29]	
G	34.75	298	Orthorh.	–	10.136	10.306	4.234	[1, 13, 40]	
H	36.0	298	Hex.	*P*3*m*1	8.453	–	21.793	[1, 13, 40]	
J	35.3	298	Hex.	–	8.373	–	10.877	[1, 13]	
K	36.05	298	Hex.	*P*3*m*1	8.328	–	7.219	[1, 13]	
K	36.2	298	Hex.	–	4.17 ± 0.02	–	21.69 ± 0.01	[41]	
Φ*	35.9	298	Monocl.	–	8.73	14.000	7.199	[13, 29]	β = 90°20'
$Cu_{3-x}Te_2$									
N_1	41.15	623	Hex.	–	20.23	–	41.19	[29, 40]	
N_2	40.15	523	Tetr.	*P*4/*nmm*	4.034	–	6.107	[29, 43, 44]	Cu_2Sb, rickardite
N_2	41.4	445	Tetr.	–	3.99	–	12.246	[28]	
N_3	41.2	293	Orthorh.	–	4.0032 ± 0.014	19.893 ± 0.007	12.220 ± 0.04	[28]	
N_3	40.8	293	Orthorh.	*Pmmm*	3.991	3.965	12.220	[40]	
N_3	40.8	298	Orthorh.	–	3.991	3.965	6.108	[29]	Cu_2Sb**
Other phases									
CuTe	50.0	298	Orthorh.	*Pmmm*	3.10	4.02	6.86	[1, 40]	Vulcanite
$CuTe_2$	66.7	298	Cubic	*Pa*3	6.600	–	–	[28]	Pyrite***

* Metastable phase.

** Partially ordered rickardite.

*** Can be prepared only at elevated pressures.

out only for Cu_2Te [48] and only at 80 K: $C_p = 31.1 \pm 2.5$ J/(mol K). Those measurements were performed with a low-temperature adiabatic calorimeter by a heat-pulse technique. The sample was prepared from high-purity copper and tellurium, but it is not clear whether its homogeneity was sufficiently high.

Given that $Cu_{2-x}Te$ exists in four polymorphs and that its homogeneity range becomes markedly narrower with decreasing temperature, $Cu_{2-x}Te$ samples for heat capacity measurements must be prepared very carefully, and the phase composition of the sample must be checked at each temperature. These points will receive special attention in analyzing heat capacity results.

The heat capacity of Cu_2Te above 298.15 K was measured in [19, 49, 50] (Fig. 6). In those studies, samples were prepared from semiconductor-grade tellurium; semiconductor-grade copper was also used in [19, 49]. Mills and Richardson [50] used 99.9%-pure

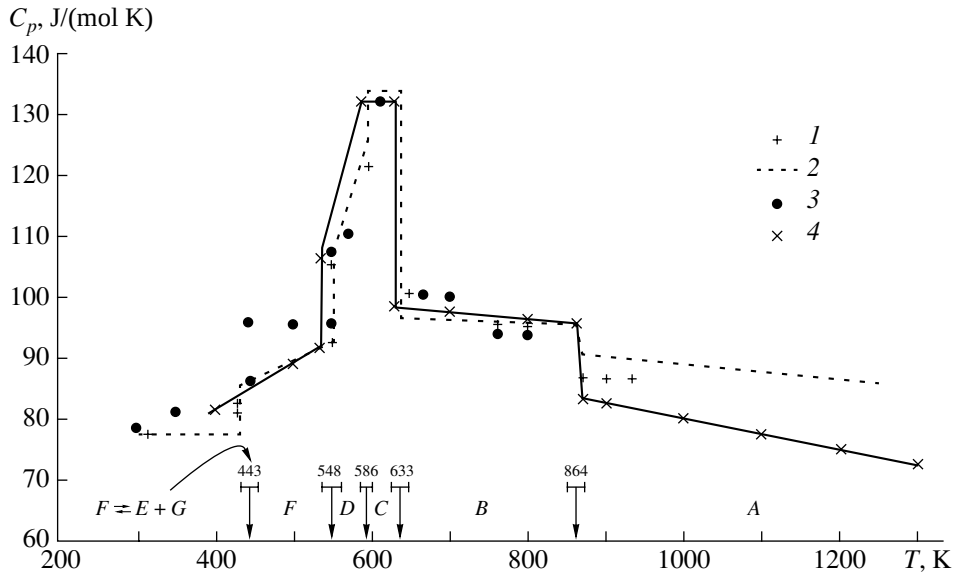

Fig. 6. Temperature-dependent heat capacity and phase transitions of Cu_2Te between 300 and 1300 K (the arrows indicate the transition temperatures): (*1*) [49], (*2*) [19], (*3*) [50], (*4*) our recommendations.

copper. Before preparing mixtures, copper was reduced in hydrogen to remove the surface oxide layer. The samples had stoichiometric compositions. Kubaschewski and Nölting [49] gave no exact details of their preparation procedure. The procedures in [19, 50] were very similar. The samples were heated stepwise to 20–35 K above the melting point of Cu_2Te. Mills and Richardson [50] held the solidified sample at 800 K for 3 days and then cooled it to room temperature over a period of 4 days. The preparation details were described in [51]. Blachnik and Gunia [19] annealed the sample for 3 weeks. The homogeneity of the samples was checked by microstructural examination or XRD [50, 51].

It follows from the heat capacity data obtained in [19, 49, 50] that the Cu_2Te samples were mixed-phase.

1. The three samples underwent a phase transition inconsistent with the equilibrium *T–x* phase diagram (Fig. 1). The parameters of that phase transition are listed in Table 6. The transition temperatures in Table 6 provide conclusive evidence that all of the samples were two-phase and contained the *G* phase below 443 K and the *F* phase above 443 K. It follows from the $\Delta_{tr}H$ data in Table 6 that the sample studied in [49] contained the smallest amount of the *G* phase at room temperature. Stoichiometric Cu_2Te (33.33 at. % Te) at 298 K would consist of (Cu) and the *E* phase, and no $F \rightleftarrows E + G$ three-phase would be detected (Fig. 2).

2. Deviations from stoichiometry can be assessed from the temperature of the $A \rightleftarrows B$ transformation. In the (Cu) + $B \rightleftarrows A$ two-phase region, the transition temperature is constant at 864 ± 15 K (Fig. 1). The temperature of the $A \rightleftarrows B$ transformation determined in the studies in question was 841 [49], 835 [19], and 750 K [50]. The reason for this discrepancy is that, within the homogeneity range of $Cu_{2-x}Te$, the reduction in transition temperature depends on composition (Fig. 2). The above temperatures of the $A \rightleftarrows B$ transformation indicate that the sample studied in [49] contained the smallest amount of excess tellurium. The sample studied in [19] was slightly more Te-rich, and the sample prepared in [50] contained the largest amount of excess Te (≃0.9 at. %). These conclusions correlate well with the above assessment of the quality of the samples studied in [19, 49] form the heat of the $F \rightleftarrows E + G$ transformation (Table 6).

3. A noteworthy feature is that the temperatures of the three-phase equilibria (Cu) + $D \rightleftarrows E$ and $D \rightleftarrows E + F$ differ little (Fig. 2).

These observations lead us to turn to the transition temperatures determined calorimetrically: 531 K in [19, 49] and 526 K in [50]. Given that the samples studied in [19, 49] contained less excess tellurium, the value T_{tr} = 531 K appears more reliable. Supposing that 531 K is the temperature of the $E \rightleftarrows D$ phase transition and taking the lower limits of the temperatures of

Table 6. "Additional" phase transition $E \rightleftarrows E'$ of Cu_2Te

T_{tr}, K	$\Delta_{tr}H$, kJ/mol	Reference
433	0.71 ± 0.11	[19]
433	0.22 ± 0.13	[49]
440	0.5	[50]
443 ± 7	–	[2, 3, 21]

Table 7. Three-phase equilibria [1] corresponding to the *A*–*E* polymorphic transformations of Cu_2Te [19, 49, 50] and heats of phase transformations

Three-phase equilibrium	*T*, K	Phase transition	T_{tr}, K	$\Delta_{tr}H$, kJ/mol	T_{tr}, K	$\Delta_{tr}H$, kJ/mol	T_{tr}, K	$\Delta_{tr}H$, kJ/mol
			[19]		[49]		[50]	
(Cu) + $D \rightleftharpoons E$	548 ± 15	$E \rightleftharpoons D$	531	1.575 ± 0.205	531	1.90 ± 0.05	526	0.5(?)
(Cu) + $C \rightleftharpoons D$	586 ± 5	$D \rightleftharpoons C$	590	0.656 ± 0.285	590	0.97 ± 0.02	600	0.5
(Cu) + $B \rightleftharpoons C$	633 ± 7	$C \rightleftharpoons B$	635	2.81 ± 0.36	635	2.45 ± 0.10	625	2.6
(Cu) + $A \rightleftharpoons B$	864 ± 15	$B \rightleftharpoons A$	835	1.415 ± 0.575	841 ± 6	2.00 ± 0.05	750(?)	2.00

the above three-phase transformations (Tables 3, 4), we obtain

$E \rightleftharpoons D$	(Cu) + $D \rightleftharpoons E$	$D \rightleftharpoons E + F$
531 ± 1 K [49]	533 K	536 K

The first two temperatures are essentially identical. It seems likely that, because of the large deviation from stoichiometry in their sample, Mills and Richardson [50] observed a combined phase transition related to the two three-phase equilibria $E \rightleftharpoons D$ and (Cu) + $D \rightleftharpoons E$, instead of the (Cu) + $D \rightleftharpoons E$ phase transition or the three-phase equilibrium $D \rightleftharpoons E + F$, since the peak in their DSC curve was rather broad and shifted to lower temperatures. Thus, the transition temperatures reported in [49, 50] and the minimum temperature of the three-phase equilibrium (Cu) + $D \rightleftharpoons E$ are essentially identical.

All of the above confirms that the heats of phase transitions determined in [49] for stoichiometric Cu_2Te are the most accurate. Table 7 compares the temperatures of the three-phase equilibria under consideration with the transition temperatures and lists the corresponding values of $\Delta_{tr}H$ [19, 49, 50].

In the studies in question, $\Delta_{tr}H$ was determined by different methods: drop calorimetry in [19], continuous-heating adiabatic calorimetry in [49], and DSC in [50]. Note that, in the heat capacity measurements in [49], essentially identical results were obtained during cooling at a rate under 0.5 K/min and during heating. The fact that the methods used in [49, 50] were dynamic makes it difficult to give preference to one of the two C_p data sets near the phase transition because, in both studies, the phase transition appeared as a peak similar to a peak in the DTA curve, which is superimposed over the $C_p(T)$ curve. The heat capacity data reported for Cu_2Te were compared in [19] graphically (see Fig. 6). Also shown in Fig. 6 are the temperature stability ranges of the *A*, *B*, *C*, *D*, and *E* phases [9, 13].

It is of interest to compare the temperatures of the polymorphic transformations $C \rightleftharpoons D$, $B \rightleftharpoons C$, and $A \rightleftharpoons B$ determined calorimetrically with the temperatures of the corresponding three-phase equilibria (Table 7). In so doing, allowance should be made that the Te-rich boundaries of the equilibria (Cu) + $C \rightleftharpoons D$ and (Cu) + $B \rightleftharpoons C$ are shifted to higher Te contents by 0.35–0.4 at. %.

Analysis of the data in Table 7 indicates that most of the results reported in [50] must be excluded from consideration. The $B \rightleftharpoons C$ transformation [49, 50] is the easiest to characterize because its temperature essentially coincides with the temperature of the three-phase equilibrium (Cu) + $B \rightleftharpoons C$. In addition, the transition temperature of 590 K [19, 49] coincides to within the experimental error with the temperature of the three-phase equilibrium (Cu) + $C \rightleftharpoons D$. In view of this, we give preference to the temperatures of these transformations reported in [19, 49]. The Te-rich boundary of the three-phase equilibrium (Cu) + $A \rightleftharpoons B$ lies at the stoichiometric composition Cu_2Te, and the temperature of this equilibrium is 864 ± 15 K (Table 3, Fig. 1). At the same time, the temperature of the $A \rightleftharpoons B$ transformation depends on composition within the homogeneity range of $Cu_{2-x}Te$. For this reason, the temperature of the $A \rightleftharpoons B$ transformation of Cu_2Te must be taken to equal the temperature of this three-phase equilibrium, i.e., 864 K, since all of the samples used in the calorimetric studies in question contained an excess of tellurium.

We note finally that the composition stability limits of the *E* phase are determined only approximately, and

Table 8. Coefficients of the best fit equations of $C_p(T)$ for Cu_2Te polymorphs between 298.15 and 1300 K

Polymorph	ΔT, K	$C_p = a + bT$	
		a	*b*
E	298.15–531	56.995	0.0645
D	531–590	−65.750	0.324
C	590–635	131.6 ± 1.0	–
B	635–864	106.088	−0.0129
A	864–1300	112.87	−0.0236

Table 9. Standard heat of formation of E-Cu_2Te determined by thermochemical methods

Method	$-\Delta_f H^0_{298}$, kJ/mol	Ref.
Dissolution in $Br_2 + H_2O$	46	[52]*
Tin calorimetry	46.55 ± 0.63	[47]
Tin calorimetry	45.66	[46]

* Since the results obtained by Fabre [52] were published in 1888, here we give the value based on the currently available data on the constituent elements [39].

it cannot be ruled out that these limits are actually closer to the stoichiometric composition Cu_2Te than is shown in the T–x phase diagram of the Cu–Te system (Fig. 1).

Figure 6 clearly demonstrates that C_p is a linear function of temperature for all the phases except C, whose heat capacity is temperature-independent. The decrease in heat capacity with increasing temperature was interpreted by Kubaschewski and Nölting [49] as due to structural disordering.

The best fit equations of $C_p(T)$ are given in Table 8.

The heat capacity of CuTe was determined in [50] by DSC in the range 266–605 K. The sample was prepared by annealing an elemental mixture at 500 K for 2 months in a tube sealed-off under vacuum.

Using the Sigma-Plot program, the results obtained in [50] were represented by the best fit equation (298–600 K)

$$C_p(T) = 74.101 - 0.125T + 2.00 \times 10^{-4}T^2. \quad (5)$$

Heat of formation of Cu_2Te: Thermochemical method. Of the many copper tellurides, the standard heat of formation was determined thermochemically for E-Cu_2Te only. More than 120 years ago, Fabre [52] synthesized crystalline Cu_2Te in an isothermal calorimeter and then oxidized it by bromine. His results were revaluated in [39] and are given in Table 9 together with tin calorimetry data [46, 47]. To reduce the results to a standard temperature (dissolution was conducted at 700 K), the heat capacity of copper was taken from [53], and that of tellurium from [54]. For copper telluride, we used the present results. Note that the data obtained in [47, 52] agree well (Table 9).

Evaluation of the thermodynamic characteristics of copper tellurides from emf measurements. The thermodynamic characteristics (standard heat of formation and standard entropy) of Cu_2Te, Cu_3Te_2, and CuTe can be extracted from emf measurements.

Such studies were carried out at the Institute of Physics, AzSSR Academy of Sciences [55, 56], and at the Laboratory of Chemical Thermodynamics, Faculty of Chemistry, Moscow State University [57, 58]. The results obtained by Abbasov *et al.* were described in grater detail in [55]. Using liquid glycerol electrolyte, they studied transport of Cu^+ dissolved in the electrolyte in a bromide form together with KBr in order to raise solubility. As electrodes, they used Cu, Te, or copper tellurides. The $\Delta_f H^0_{298}$ and $\Delta_f S^0_{298}$ calculated for the formation of copper tellurides from Cu and Te are listed in Table 10. The calculated $\Delta_f S^0_{298}$ and reference data from [37, 38] were used to evaluate S^0_{298} (Table 10).

Gerasimov *et al.* [57, 58] measured emf by a high-speed method, using an aqueous $CuCl_2$ solution as an electrolyte and $Cu|CuCl_2 aq|Cu_xTe_{1-x}$ electrochemical cells. The electrode process was shown to be due to Cu^+ transport. Measurements were made in the temperature range 293–353 K, which is half as broad as that in [55] (300–420 K). Accordingly, the errors in emf measurements, $\Delta_f H^0_{298}$, and $\Delta_f S^0_{298}$ were larger than those in [55, 56]. Clearly, the data obtained in [55] are more reliable. Note that, in all studies, the composition of Cu_xTe_{1-x} samples was Cu_4Te_3. Since the potential-forming reaction was $Cu^0 - e \longrightarrow Cu^+$, and the actual electrode composition was Cu_3Te_2 + CuTe or Cu_2Te + Cu_3Te_2, the results of emf measurements and ΔG, ΔH, and ΔS calculations can be used to evaluate the thermodynamic characteristics of Cu_3Te_2. Remarkably, the XRD studies of copper tellurides reported by Shifizade [59] revealed the formation of Cu_3Te_2 + CuTe two-phase samples, while Cu_4Te_3 was not detected.

Table 10. Standard heats of formation and standard entropies of copper tellurides evaluated from emf data

Compound	$-\Delta_f H^0_{298}$, kJ/mol	$\Delta_f S^0_{298}$, J/(mol K)	S^0_{298}, J/(mol K)	$-\Delta_f H^0_{298}$, kJ/mol	$\Delta_f S^0_{298}$, J/(mol K)	S^0_{298}, J/(mol K)
	[55]			[57, 58]		
CuTe	23.6 ± 3.0	2.89 ± 0.84	85.5 ± 2.3	23.2 ± 2.9	6.2 ± 9.3	88.8 ± 9.3
Cu_3Te_2	76.6 ± 5.4	–11.59 ± 0.90	186.9 ± 2.7	75.7 ± 1.04	–5.98 ± 3.71	192.5 ± 3.7
E-Cu_2Te	45.1 ± 2.9	4.81 ± 0.84	120.6 ± 2.3	44.8 ± 2.5	7.75 ± 14.8	123.6 ± 14.9

Table 11. Thermodynamic properties of Cu_2Te

Phase	T, K	C_p, J/(mol K)	$H^0 - H^0_{298}$, J/mol	$S^0 - S^0_{298}$, J/(mol K)	S^0_T, J/(mol K)	Φ''_T, J/(mol K)
E	298	76.22	0	0	120.6 ± 2.3	120.6 ± 2.3
	400	82.80	8098	23.3	144	124
	500	89.24	16700	42.5	163	130
	531	91.24	19498	48.0	169	132
D	531	106.30	21398	51.6	172	132
	590	125.41	28233	63.79	184	136
C	590	131.60	29203	65.4	186	136
	635	131.60	35125	75.07	196	140
B	635	97.90	37575	78.8	199	140
	700	97.06	43911	88.3	209	146
	800	95.77	53552	101.2	222	155
	864	94.94	59655	108.5	229	160
A	864	83.21	61655	110.8	231	160
	900	82.28	64634	114.2	235	163
	1000	79.70	72733	126.2	247	174
	1100	77.12	80574	130.4	251	177
	1200	74.54	88157	136.7	257	184
	1300	71.96	95482	142.8	263	190

The evaluation of the thermodynamic characteristics of Cu_2Te was based on the potential-forming reaction

$$1/2Cu + 1/2Cu_3Te_2 \rightleftharpoons Cu_2Te. \quad (6)$$

In the phase diagram, Cu_2Te and Cu_2Te_2 are separated by the intermediate phases *G*, *J*, and *K* (Fig. 2), which are left out of consideration in calculating the thermodynamic characteristics of Cu_2Te. Nevertheless, the standard heat of formation calculated from emf data (Table 10) agrees well with the heat of formation of Cu_2Te evaluated by thermochemical methods (Table 9). It seems likely that the energy contribution of the *G*, *J*, and *K* phases to the equilibria in question is rather small.

Thermodynamic characteristics of Cu_2Te and CuTe. The thermodynamic properties of Cu_2Te polymorphs (*E*–*A*) evaluated from heat capacity data (Tables 7, 8, 10) are summarized in Table 11.

CONCLUSIONS

We analyzed the *T*–*x* phase diagram of the Cu–Te system; heat capacity data for Cu_2Te and CuTe; calorimetrically determined heats of formation of Cu_2Te and CuTe; and heats of formation and standard entropies of Cu_2Te, Cu_3Te_2, and CuTe evaluated from emf measurements. However, this review is not comprehensive.

First, we did not consider data on the dissociation pressures of copper tellurides. Although this issue was addressed in a number of publications [51, 60, 61, 62], further research is needed because Te vapor has a complex composition [38, 50, 54, 63].

Second, there is great interest in mapping out the *p*–*T* phase diagram of the Cu–Te system using the currently available *T*–*x* phase-diagram data. Some headway has already been made on this problem [64–66].

ACKNOWLEDGMENTS

We are grateful to S.V. Nikolashin, V.N. Potolokov, I.B. Kutsenok, and A.M. Savina for their assistance with this study.

REFERENCES

1. Okamoto, H., Cu–Te (Copper–Tellurium), *Phase Diagrams of Binary Copper Alloys*, Subramanian, P.R. *et al.*, Eds., Materials Park: American Society for Metals, 1994, pp. 434–439.
2. Feutelias, Y. and Legendre, B., Binary Phase Diagrams of Tellurium and Posttransitional Elements (I B, II B,

III B, IV B, V B, VI B), *Thermochim. Acta*, 1998, vol. 313, no. 1, pp. 35–53.

3. Cu–Te (Copper–Tellurium), *Alloys Phase Diagrams*, Massalski, Th.B., Ed., Materials Park: American Society for Metals, 1990, vol. 2, pp. 1490–1492.
4. Regel', A.R. and Glazov, V.M., *Fizicheskie svoistva elektronnykh rasplavov* (Physical Properties of Electronic Melts), Moscow: Nauka, 1980.
5. Buketov, E.A. and Malyshev, V.P., *Izvlechenie selena i tellura iz med'elektrolitnykh shlamov* (Extraction of Selenium and Tellurium from Cupriferous Electrolyte Slime), Almaty: Nauka, 1969.
6. Puschin, N.A., Potential and Nature of Metallic Alloys, *Zh. Ross. Khim. O–va. im. D. I. Mendeleeva*, 1907, vol. 39, part 1, pp. 13–54.
7. Puschin, N.A., Das Potential und die chemische Konstitution der Metall-Legirungen, *Z. Anorg. Allg. Chem.*, 1907/1908, vol. 56, no. 1, pp. 1–45.
8. Chikashige, M., Metallographische Mitteilungen aus dem Institut für anorganische Chemie der Universität Göttingen: XLV. Über Kupfer–Tellur, *Z. Anorg. Allg. Chem.*, 1907, vol. 54, no. 1, pp. 50–57.
9. Keymling, O., *Dissertation*, Bergakademie Clausthal, 1952.
10. Hansen, M. and Anderko, K., *Constitution of Binary Alloys*, New York: McGraw–Hill, 1957. Translated under the title *Struktury dvoinykh splavov*, Moscow: Metallurgizdat, 1962, pp. 682–684.
11. Gravemann, H. and Wallbaum, H.-J., Zur Kenntnis des Dreistoffsystems Kupfer–Blei–Tellur, *Z. Metallkd.*, 1956, vol. 47, no. 6, pp. 433–441.
12. Anderko, K. and Schubert, K., Untersuchungen im System Kupfer–Tellur, *Z. Metallkd.*, 1954, vol. 45, no. 6, pp. 371–378.
13. Blachnik, R., Lasocka, M., and Walbrecht, U., The System Copper–Tellurium, *J. Solid State Chem.*, 1983, vol. 48, no. 3, pp. 431–438.
14. Glazov, V.M., Pavlova, L.M., and Asryan, A.A., Thermal Dissociation of Copper Chalcogenides during Melting, *Zh. Fiz. Khim.*, 1996, vol. 70, no. 2, pp. 232–236.
15. Glazov, V.M., Kim, S.G., and Nurov, K.B., Acoustic Study of the Binodal Bounding the Liquid–Liquid Equilibrium in the Cu–Te System, *Zh. Fiz. Khim.*, 1990, vol. 64, no. 7, pp. 1985–1987.
16. Burylev, B.P., Fedorova, N.N., and Tsemekhman, L.Sh., Cu–S, Cu–Se, and Cu–Te Phase Diagrams, *Zh. Neorg. Khim.*, 1974, vol. 19, no. 8, pp. 2283–2285.
17. Burylev, B.P., Tsemekhman, L.Sh., and Fedorova, N.N., Sulfur, Selenium, and Tellurium Activities in Liquid Copper, *Zh. Fiz. Khim.*, 1975, vol. 49, no. 12, p. 3112.
18. Glazov, V.M. and Mendelevich, A.Yu., Entropy of Melting of Silver and Copper Chalcogenides, *Elektron. Tekh., Ser. 14: Mater.*, 1968, no. 1, pp. 114–119.
19. Blachnik, R. and Gunia, P.-G., Enthalpien von Kupfer- und Silberchalkogeniden, *Z. Naturforsch. A*, 1978, vol. 33, no. 1, pp. 114–119.
20. Glazov, V.M., Burkhanov, A.S., and Saleeva, N.M., Preparation of Single-Phase Copper and Silver Chalcogenides, *Izv. Akad. Nauk SSSR, Neorg. Mater.*, 1977, vol. 13, no. 5, pp. 917–918.
21. Pashinkin, A.S., Pavlova, L.M., and Amirov, R.A., *p–T* Phase Diagram of the Copper–Tellurium System, *Izv. Akad. Nauk SSSR, Neorg. Mater.*, 1985, vol. 21, no. 12, pp. 2088–2089.
22. Belousov, A.A., Bakhvalov, S.G., Aleshina, S.N., *et al.*, *Fiziko-khimicheskie svoistva zhidkoi medi i ee splavov: Spravochnik* (Physicochemical Properties of Liquid Copper and Its Alloys: A Handbook), Yekaterinburg: Inst. Metallurgii Ural. Otd. Ross. Akad. Nauk, 1997.
23. Burton, P.B. and Skinner, B.J., Stability of Sulfide Minerals, *Geochemistry of Hydrothermal Ore Deposits*, Barns, H.L., Ed., New York: Wiley, 1979. Translated under the title *Geokhimiya gidrotermal'nykh rudnykh mestorozhdenii*, Moscow: Mir, 1982, pp. 238–327.
24. Glazov, V.M., Pashinkin, A.S., and Fedorov, V.A., Phase Equilibria in the Cu–Se System, *Neorg. Mater.*, 2000, vol. 36, no. 7, pp. 775–783 [*Inorg. Mater.*, (Engl. Transl.), vol. 36, no. 7, pp. 641–652].
25. Miyatani, S., Mori, S., and Yanagihara, M., Phase Diagram and Electrical Properties of $Cu_{2-x}Te$, *J. Phys. Soc. Jpn.*, 1979, vol. 47, no. 4, pp. 1152–1158.
26. Gustaviano, F., Luquet, H., and Bouguot, J., Du diagramme du phase du systeme Cu–Te dans le ine de la solution solid $Cu_{2-x}Te$ ($0 < x < 0.16$), *Mater. Res. Bull.*, 1973, vol. 8, pp. 935–942.
27. Sharma, I.B. and Selekna, B., Study of Transformations in Copper Telluride, *Indian J. Chem., A*, 1989, vol. 28, no. 1, pp. 16–18.
28. Misota, T., Koto, K., and Morimoto, N., Crystallography and Composition of Synthetic Rickardite, *Mineral. J.*, 1973, vol. 7, no. 3, pp. 252–261.
29. Stevels, A.L.N., Phase Transitions in Nickel and Copper Selenides and Tellurides, *Philips Res. Rep. Suppl.*, 1969, no. 9, p. 124.
30. Stevels, A.L.N. and Wiegers, G.A., Phase Transition in Copper Chalcogenides: 2. The Tellurides $Cu_{3-x}Te_2$ and CuTe, *Rec. Trav. Chim. Pay-Bas*, 1971, vol. 90, pp. 352−359.
31. Lorenz, G. and Wagner, C., Investigation on Cuprous Selenide and Telluride, *J. Chem. Phys.*, 1957, vol. 26, no. 6, pp. 1607–1608.
32. Burmeister, J., Beobachtungen zur Polymorphie des Ricardits Cu_4Te_3, *Z. Metallkd.*, 1966, vol. 57, no. 4, pp. 325–326.
33. Colaitis, D., Van Dyck, D., Delavignette, P., *et al.*, High-Resolution Electron Microscopic and Electron Diffraction Study of Non-Stoichiometric Phase in $Cu_{3-x}Te_2$, *Phys. Status Solidi A*, 1980, vol. 58, no. 1, pp. 271–288.
34. Tonkov, E.Yu., *Fazovye prevrashcheniya soedinenii pri vysokikh davleniyakh: Spravochnik* (High-Pressure Phase Transformations of Compounds: A Handbook), Moscow: Metallurgiya, 1988, part 1.
35. Smart, J.S. and Smith, A.A., Effect of Certain Fifth Period Elements on Some Properties of High Purity Copper, *Trans. AIME*, 1949, vol. 152, no. 1, pp. 103–117.
36. Eborall, R., Some Observation on the Mode of Occurrence of Selenium, Tellurium, and Bismuth in Copper, *J. Inst. Met.*, 1944, vol. 70, pp. 435–446.
37. *Termicheskie konstanty veshchestv. Spravochnik* (Thermal Constants of Substances: A Handbook), Glushko, V.P., Ed., Moscow: VINITI, 1972, issue VI, part 1.

38. *Termicheskie konstanty veshchestv. Spravochnik* (Thermal Constants of Substances: A Handbook), Glushko, V.P., Ed., Moscow: VINITI, 1966, issue II.

39. Lonadi, S., Yassin, A., Bros, H., *et al.*, Thermodynamic Investigation of the Ag–Te and Cu–Te Eutectic Alloys, *J. Alloys Compd.*, 1995, vol. 224, no. 1, pp. 351–354.

40. Villars, P. and Calvert, L.D., *Pearson's Handbook of Crystallographic Data for Intermetallic Phases*, Metals Park: American Society for Metals, 1985, vol. 2.

41. Asadov, Yu.G., Rustamova, L.V., Gasimov, G.B., *et al.*, Structural Phase Transition in $Cu_{2-x}Te$ Crystals (x = 0.00; 0.10; 0.15; 0.20; 0.25), *Phase Transitions, Ser. A*, 1992, vol. 38, no. 4, pp. 247–259.

42. Tsypin, M.I. and Chipizhenko, A.A., Structure and Properties of the Lower Copper Telluride, *Izv. Akad. Nauk SSSR, Neorg. Mater.*, 1974, vol. 10, no. 7, pp. 1210–1214.

43. Forman, S.A. and Peacock, M.A., Crystals Structure of Rickardite $Cu_{4-x}Te_2$, *Am. Mineral.*, 1949, vol. 34, pp. 441–451.

44. Patzak, I., Über die Struktur und die Lage der Phasen im System Kupfer–Tellur, *Z. Metallkd.*, 1956, vol. 47, no. 6, pp. 418–420.

45. Baranova, R.V. and Pinsker, Z.G., Disordering of the Tetragonal Phase $Cu_{4-x}Te_2$, *Kristallografiya*, 1969, vol. 14, no. 2, pp. 274–278.

46. Chizhikov, D.M. and Schastlivyi, V.P., *Tellur i telluridy* (Tellurium and Tellurides), Moscow: Nauka, 1966.

47. Vecher, A.A., Mechkovskii, L.A., and Skoropanov, A.S., Heat of Formation of Some Tellurides, *Izv. Akad. Nauk SSSR, Neorg. Mater.*, 1974, vol. 10, no. 2, pp. 2140–2143.

48. Gul'tyaev, P.V. and Petrov, A.V., Heat Capacity of Some Semiconductors, *Fiz. Tverd. Tela* (Leningrad), 1959, vol. 1, no. 3, pp. 368–372.

49. Kubaschewski, P. and Nölting, J., Spezifische Warmen und termische Felhordnung von Kupferchalkageniden: Teil I, *Ber. Bunsen-Ges. Phys. Chem.*, 1973, vol. 77, pp. 70–74.

50. Mills, K.C. and Richardson, M.J., The Heat Capacity of Cu_2Te(c), CuTe(c), Ag_2Te(c), $Ag_{1.9}Te$(c), and $Ag_{1.64}Te$(c), *Thermochim. Acta*, 1973, vol. 6, pp. 427–438.

51. Mills, K.C., The Dissociation Pressure and Thermodynamic Properties of Cu_2Te(c), Ag_2Te(c), $Ag_{1.9}Te$(c), and $Ag_{1.64}Te$(c), *J. Chem. Thermodyn.*, 1972, vol. 4, no. 9, pp. 903–913.

52. Fabre, C., Tellurures métalliques cristallines, *Ann. Chim. Phys., Ser. 6*, 1888, pp. 110–120.

53. Wicks, C.E. and Block, F.E., *Thermodynamic Properties of 65 Elements—Their Oxides*, Halides, Carbides, and Nitrides, *Bull.—U.S., Bur. Mines*, 1963, no. 605. Translated under the title *Termodinamicheskie svoistva 65 elementov, ikh okislov, galogenidov, karbidob i nitridov*, Moscow: Metallurgiya, 1965.

54. Gerasimov, Ya.I., Krestovnikov, A.N., and Gorbov, S.I., *Khimicheskaya termodinamika v tsvetnoi metallurgii* (Chemical Thermodynamics in Nonferrous Metallurgy), Moscow: Metallurgiya, 1974.

55. Abbasov, A.S., Azizov, T.Kh., Alieva, N.A., *et al.*, *Issledovanie termodinamicheskikh svoistv telluridov medi* (Thermodynamic Study of Copper Tellurides), Available from VINITI, 1976, 1587-76

56. Abbasov, A.S., *Termodinamicheskie svoistva nekotorykh poluprovodnikovykh sistem* (Thermodynamic Properties of Some Semiconductor Systems), Baku: Elm, 1981.

57. Gerasimov, Ya.I., Kutsenok, I.B., and Geiderikh, V.A., Thermodynamic Studies of Copper Tellurides by High-Speed EMF Measurements, in *Ya.I. Gerasimov. Izbrannye trudy* (Ya.I. Gerasimov: Selected Works), Moscow: Nauka, 1988, pp. 327–330.

58. Gerasimov, Ya.I., Kutsenok, I.B., and Geiderikh, V.A., Thermodynamic Studies of Copper Tellurides by High-Speed EMF Measurements, in *Termodinamika i poluprovodnikovye materialy* (Thermodynamics and Semiconductor Materials), Moscow: Mosk. Inst. Elektronnoi Tekhniki, 1980, pp. 110–114.

59. Shifizade, R.B., *Fazoobrazovanie i kinetika fazovykh prevrashchenii v tonkikh plenkakh A^I–B^{VI}* (Phase Formation and Transformation Kinetics in Thin I–VI Films), Baku: Elm, 1983.

60. Malkova, A.S., Pashinkin, A.S., and Amirov, R.A., Heat of Formation of Cu_2Te, *Elektron. Tekh., Ser. 6: Mater.*, 1984, no. 10 (195), pp. 43–44.

61. Glazov, V.M., Pashinkin, A.S., Malkova, A.S., and Belyak, A.F., Dissociation Pressure of Cu_2Te, *Izv. Akad. Nauk SSSR, Neorg. Mater.*, 1980, vol. 19, no. 9, pp. 1522–1525.

62. Korenchuk, N.M. and Tishchenko, I.A., Copper Chalcogenide Systems: Phase Diagrams and Mass Spectrometric Studies of Vapor Composition and Pressure, *Zh. Fiz. Khim.*, 1997, vol. 17, no. 11, pp. 1932–1936.

63. Gurvich, L.V., IVTANTERMO—Thermodynamic Properties Database, *Elektron. Tekh., Ser. 6: Mater.*, 1974, no. 9 (84), pp. 36–41.

64. Pashinkin, A.S., Pavlova, L.M., and Amirov, R.A., *p–T* Phase Diagrams of the Systems Copper–Tellurium and Copper Selenium, *Elektron. Tekh., Ser. 6: Mater.*, 1985, no. 1, p. 52.

65. Pashinkin, A.S., Pavlova, L.M., and Amirov, R.A., *p–T* Phase Diagram of the System Copper–Tellurium, *Izv. Akad. Nauk SSSR, Neorg. Mater.*, 1985, vol. 21, no. 12, pp. 2088–2091.

66. Levinskii, Yu.V., *p–T–x-diagrammy sostoyaniya dvoinykh metallicheskikh sistem: Spravochnik* (*P–T–x* Phase Diagrams of Binary Metallic Systems), Moscow: Metallurgiya, 1990.